OFFICE OF NAVAL RESEARCH

Contract N00014-82K-0612

Task No. NR 627-838

TECHNICAL REPORT NO. 31

A Fresh Look at Transport in Perfluorosulfonate Ionomers: Ultramicroelectrode Investigations of Nafion and Dow Ionomers

by

Lisa D. Whiteley and Charles R. Martin

Prepared for publication

in

The Journal of Physical Chemistry

Department of Chemistry
Texas A&M University
College Station, TX 77843

January 11, 1989

UNCLASSIFIED

SECURITY CLASSIFICATION OF THIS PAGE (When Data Entered)

REPORT DOCUMENTATION PAGE

READ INSTRUCTIONS BEFORE COMPLETING FORM

1. REPORT NUMBER: Technical Report # 31	2. GOVT ACCESSION NO.: AD-A203 555
3. RECIPIENT'S CATALOG NUMBER:	
4. TITLE (and Subtitle): "A Fresh Look at Transport in Perfluorosulfonate Ionomers: Ultramicroelectrode Investigations of Nafion and the Dow Ionomers"	5. TYPE OF REPORT & PERIOD COVERED: Technical Report
	6. PERFORMING ORG. REPORT NUMBER:
7. AUTHOR(s): Lisa D. Whiteley and Charles R. Martin	8. CONTRACT OR GRANT NUMBER(s): N00014-82K-0612
9. PERFORMING ORGANIZATION NAME AND ADDRESS: Department of Chemistry, Texas A&M University, College Station, TX 77843	10. PROGRAM ELEMENT, PROJECT, TASK AREA & WORK UNIT NUMBERS: NR 627-838
11. CONTROLLING OFFICE NAME AND ADDRESS: Office of Naval Research, 800 North Quincy Street, Arlington, VA 22217	12. REPORT DATE: January 11, 1989
	13. NUMBER OF PAGES:
14. MONITORING AGENCY NAME & ADDRESS(if different from Controlling Office):	15. SECURITY CLASS. (of this report): UNCLASSIFIED
	15a. DECLASSIFICATION/DOWNGRADING SCHEDULE:

16. DISTRIBUTION STATEMENT (of this Report)

APPROVED FOR PUBLIC DISTRIBUTION, DISTRIBUTION UNLIMITED

17. DISTRIBUTION STATEMENT (of the abstract entered in Block 20, if different from Report)

18. SUPPLEMENTARY NOTES

19. KEY WORDS (Continue on reverse side if necessary and identify by block number)

Perfluorosulfonate Ionomers; ~~Ultra~~microelectrode; Nafion; Dow Ionomers; Chronoamperometry; Apparent diffusion coefficients, Sulfonates. (Mgm)

20. ABSTRACT (Continue on reverse side if necessary and identify by block number)

Chronoamperometry at ultramicroelectrodes is a powerful and convenient technique for the determination of apparent diffusion coefficients and concentrations of electroactive cations ion-exchanged into Nafion and Dow perfluorosulfonate films. This technique offers tremondous advantages over the conventional electrochemical methods which employ film-coated macro-sized electrodes. These advantages stem from the elimination of iR distortion at the ultramicroelectrode and from the ability to determine

(continued)

DD FORM 1 JAN 73 1473 EDITION OF 1 NOV 65 IS OBSOLETE

S/N 0102-LF-014-6601

UNCLASSIFIED

SECURITY CLASSIFICATION OF THIS PAGE (When Data Entered)

(Abstract continued)

both the concentration and apparent diffusion coefficient of the electroactive cation from a single experiment. Further improvements over the conventional approach were achieved by eliminating coupled diffusion and migration contributions to the measured current response. Under these conditions, charge is transported via ionic diffusion rather than through electron hopping. Furthermore, the apparent diffusion coefficients decrease with increasing concentration of the electroactive cation in the film. This decreasing diffusion coefficient with increasing concentration was attributed to a bottleneck effect caused by the narrow channels which interconnect the ionic clusters in these ionomers.

(2)

Contract N00014-82-K-0612

A Fresh Look at Transport in Perfluorosulfonate Ionomers: Ultramicroelectrode Investigations of Nafion and the Dow Ionomers

Lisa D. Whiteley and Charles R. Martin*

Department of Chemistry
Texas A&M University
College Station, TX 77843

*To whom correspondence should be addressed.

3

Abstract

Chronoamperometry at ultramicroelectrodes is a powerful and convenient technique for the determination of apparent diffusion coefficients and concentrations of electroactive cations ion-exchanged into Nafion and Dow perfluorosulfonate films. This technique offers tremendous advantages over the conventional electrochemical methods which employ film-coated macro-sized electrodes. These advantages stem from the elimination of iR distortion at the ultramicroelectrode and from the ability to determine both the concentration and apparent diffusion coefficient of the electroactive cation from a single experiment. Further improvements over the conventional approach were achieved by eliminating coupled diffusion and migration contributions to the measured current response. Under these conditions, charge is transported via ionic diffusion rather than through electron hopping. Furthermore, the apparent diffusion coefficients decrease with increasing concentration of the electroactive cation in the film. This decreasing diffusion coefficient with increasing concentration was attributed to a bottleneck effect caused by the narrow channels which interconnect the ionic clusters in these ionomers.

Introduction

Perfluorosulfonate ionomers (PFSI's) are unique ion-exchange materials with outstanding chemical and thermal stabilities (1). Du Pont's Nafion polymers (Structure I in Figure 1) are the most widely investigated PFSI's; the Dow Chemical Company has recently described a related series of PFSI's (Structure II in Figure 1). Current applications of PFSI's include use in chlor-alkali cells (2), fuel cells (3), batteries (4) and water electrolyzers (5). All of these applications involve ion or charge-transport through a film or membrane of the polymer. Results of numerous investigations of the rates and mechanisms of charge-transport in PFSI films and membranes have appeared in the recent literature (6,7).

One approach for evaluating the transport properties of PFSI's involves electrochemical determinations of apparent diffusion coefficients, D_{app}'s, for electroactive cations ion-exchanged into the polymer (7). Typically, these D_{app}'s are obtained by conducting potential step experiments at conventional macro-sized electrode surfaces coated with thin films of the polymer. These methods are plagued with problems and pitfalls including the need to independently determine the concentration of the electroactive cation (7), distortion of the electrochemical transient by resistance effects (8), and problems associated with migration and coupled diffusion (9).

We recently described a much simpler and less problematic approach for evaluating the transport properties of PFSI's (10). This approach involves chronoamperometric experiments at a PFSI film-coated ultramicroelectrode and provides both the apparent diffusion coefficient and the concentration (C) from a single experiment (10,11). This method is based on pioneering work by

Osteryoung et al. (12) and Oxenham et al. (11).

We have previously reported the use of this ultramicroelectrode-based method to determine both D_{app} and C for O_2 in Nafion (10). More recently, we have been using this technique to study the transport of two electroactive cations, ferrocenylmethyl trimethylammonium and $Fe(bpy)_3^{2+}$ (bpy = 2,2'-bipyridine) in Nafion and Dow PFSI films coated onto ultramicroelectrode surfaces. These studies have allowed for detailed assessments of the effects of C on the magnitude of D_{app} in the Nafion and Dow PFSI's. We report the results of these and related investigations in this paper.

Experimental

Materials - 1100 equivalent weight Nafion was obtained from duPont. 803, 909, and 1076 equivalent weight (EW) Dow PFSI was generously donated by the Dow Chemical Co. Solutions of the Nafion and Dow PFSI's were prepared as described previously; 50:50 ethanol:water served as the solvent (13). Ferrocenylmethyl trimethylammonium hexafluorophosphate ($FA^+PF_6^-$) was prepared from the iodide salt (Pfaltz and Bauer) as described previously (14). All other chemicals were used as received. A solution of 1 M NaCl served as supporting electrolyte for the ionomer film-coated ultramicroelectrode studies. All solutions were prepared using water which had been circulated through a Milli-Q water purification system (Millipore).

Ultramicroelectrode Preparation - Ultramicroelectrodes were prepared by sealing 10 μm Pt wire (Goodfellow Metals, Ltd., UK) into 5 mm od soft glass tubing as described elsewhere (10). Prior to use, the ultramicroelectrodes were polished with 0.05 micron alumina. The radii of these electrodes were determined voltammetrically (15) from plots of the steady-state current vs.

concentration for a system with a known diffusion coefficient (5 mM $Fe(CN)_6^{4-}$ in 1 M KCl at pH = 2.7 (16)).

Film-Coating Procedures - The conventional method for preparing a PFSI film-coated electrode entails depositing an aliquot of the PFSI solution onto the electrode surface and then allowing the solvent to evaporate at room temperature (7d,14). We have shown that the resulting films have poor physical strength and mechanical properties and are soluble in a variety of polar, organic solvents (17-19). We refer to this form of the polymer as "recast" PFSI (17-19).

In addition to having poor mechanical properties and high solubilities, we have shown that recast PFSI does not adhere well to glass (10,20). In order to obtain strongly adherent recast Nafion films, the glass surface surrounding the ultramicroelectrode had to be derivatized as described previously (20). (Trimethoxysilylpropyl)-N,N,N-trimethylammonium chloride was used as the derivatizing agent. After derivatization, the ultramicroelectrode tip (which includes the Pt electrode and the surrounding glass) was drop-coated with 3.00 μl of a 3.34% Nafion solution. The solvent was allowed to evaporate at room temperature, leaving a Nafion film which covered both the Pt ultramicroelectrode disk and the surrounding glass insulator.

We have recently described a high temperature solution-casting procedure which yields a PFSI film which has good mechanical properties and is insoluble in all solvents below ca. 200° C (10,17-19). This high temperature solution-cast polymer (called "solution-processed" PFSI) is essentially identical to the as-received polymer membrane. Furthermore, solution-processed PFSI adheres strongly to glass, provided the surface is

roughened (10). Solution-processed Nafion film-coated ultramicroelectrodes were prepared as follows.

Prior to coating, the glass insulator surrounding the Pt ultramicrodisk was roughened by abrading with 600 grit Carbimet paper (Buehler). 4.49 μl of a 2.23% Nafion solution in 1:1:1 ethanol:water:triethylphosphate solution were then applied to the ultramicroelectrode tip (17). The solvent was evaporated at 180°C, as described elsewhere (10).

This high temperature solution-casting procedure was also used to cast films of the Dow PFSI's onto ultramicroelectrode surfaces (19). 2.20 μl of a 4.90% Dow PFSI solution in 1:1:1 ethanol:water:triethylphosphate were applied to the ultramicroelectrode tip. As was the case with solution-processed Nafion, the solvent was evaporated at 180° C (10,17,19). After coating, all ionomer film-coated ultramicroelectrodes were equilibrated (overnight) in 1 M NaCl.

Instrumentation - The electrochemical cell and measuring circuit are shown schematically in Figure 2. The output potential of a CV-27 voltammogram (Bioanalytical Systems, Inc.) served as the waveform generator. The picoammeter was a Keithley 617 Programmable Electrometer. An Omnigraph 2000 X-Y recorder (Houston Instruments) and an Explorer III digital oscilloscope (Nicolet) were used to record the data. The oscilloscope was interfaced to a Personal System/2 Model 30 computer (IBM) via a RS-232 interface (Nicolet). The picoammeter and two-electrode electrochemical cell were housed in a Faraday cage. A saturated calomel reference electrode was used.

Electrochemical Methods - Both cyclic voltammetry and chronoamperometry were used to investigate the ionomer film-coated ultramicroelectrodes. D_{app}'s and C's for FA^+ and $Fe(bpy)_3^{2+}$ in Nafion films and D_{app}'s and C's for FA^+ in Dow

PFSI films were determined chronoamperometrically (10,11). Osteryoung derived rigorous expressions for the chronoamperometric response of the stationary disk ultramicroelectrode (12). Based on this work, Oxenham et al. developed a simplified data analysis method which allowed for the determination of both the diffusion coefficient and the concentration of the electroactive species from the chronoamperometric experiment at the ultramicroelectrode (11). We extended this method to film-coated ultramicroelectrodes (10). This method is briefly reviewed below.

The potential of the ionomer film-coated ultramicroelectrode is stepped from a value where no oxidation or reduction of electroactive species occurs, to a potential where the oxidation or reduction rate is diffusion-controlled. At short times, the diffusion-limited current is given by (12a):

$$i = \frac{2nFD_{app}Cr\pi^{1/2}}{\tau^{1/2}} + nFD_{app}Cr\pi \qquad (1)$$

where r is the ultramicroelectrode radius and n is the number of electrons transferred. The dimensionless parameter, τ, is given by (12a):

$$\tau = \frac{4D_{app}t}{r^2} \qquad (2)$$

where t is time. When τ is less than 0.8, Equation 1 is a valid approximation (within 5%) to the exact current expression (11).

According to Equation 1, a plot of i vs. $t^{-1/2}$ yields a slope proportional to $D_{app}^{1/2}C$ and an intercept proportional to $D_{app}C$. Therefore, both D_{app} and C can be obtained from a single potential step experiment. As will be discussed, in detail below, application of this method to the film-

coated ultramicroelectrode requires that the diffusion layer created at the electrode/film interface is always thinner than the film.

Procedures - Prior to electrochemical analysis, the desired electroactive cation was ion-exchanged into the ionomer film. This was accomplished by equilibrating the ultramicroelectrode overnight in a solution which was 0.1 to 1 mM in FA^+ or $Fe(bpy)_3^{2+}$ and 1 M in NaCl. Due to the high concentration of Na^+ in these solutions, only a small quantity of the electroactive cation ion-exchanged into the film. (Solutions containing electroactive cation are referred to here as "loading" solutions. The films into which these cations are exchanged are termed "loaded" films.)

Cyclic voltammetric experiments were conducted on the freshly loaded films. A scan rate of 5 mVs^{-1} was used. The potential step data were then obtained. Potential steps from +0.25 to +0.55 V (for FA^+) or from +0.65 to +0.95V (for $Fe(bpy)_3^{2+}$) were applied and the resulting current transients were recorded. These transients contained both faradaic and non-faradaic currents. The faradaic component was isolated by conducting analogous experiments at unloaded films and subtracting these non-faradaic transients from the total current transient.

The faradaic current was plotted vs. $t^{-1/2}$. D_{app}'s and C's for the electroactive cations were calculated via (11):

$$D_{app} = \frac{A^2 r^2}{\pi B^2} \tag{3}$$

and

$$C = \frac{B^2}{nFAr^3} \tag{4}$$

where A and B are the intercept and slope, respectively, of the i vs. $t^{-1/2}$ plots.

To evaluate the effect of concentration on D_{app}, a loaded, ionomer film-coated ultramicroelectrode was placed in a loading solution containing a higher concentration of the electroactive cation and allowed to re-equilibrate overnight. This allowed for additional electroactive cation to partition into the film. D_{app} and C were then redetermined as described above. This process of loading with electroactive cation followed by chronoamperometric determination of D_{app} was repeated until the desired quantity of D_{app} vs. C data was obtained.

Note that both of the electroactive cations used in these investigations are hydrophobic. We have previously shown that the water content of Nafion film decreases when a hydrophobic cation is ion-exchanged into the film (21). Thus, when the electroactive cations used here are exchanged into the PFSI's, the film water contents drop (see Figure 9); this effect could confound our attempts to determine the effect of concentration on D_{app}. For this reason, we conducted an independent evaluation of the effect of FA^+ concentration in Nafion membrane on the equilibrium water content of the membrane. The following procedure was used:

Nafion membranes were equilibrated in aqueous solutions containing varying concentrations of FA^+; these solutions contained no supporting electrolyte. Because a competing cation was not present, and because the Nafion/water partition coefficient for FA^+ is enormous (14), all of the FA^+ present in the solution partitioned into the Nafion membrane. Therefore, the quantity of FA^+ present in the membrane was precisely known.

The membranes were allowed to equilibrate with the FA^+ solutions for 3

days. After equilibration, the membranes were removed from the solutions, blotted dry with a Kim-wipe, and weighed in tared vials. The membranes were then placed in a vacuum oven at 150° C for 3 days (22). The dried membranes were then reweighed and the weight water was determined by difference. An analogous procedure was used to determine the water content of FA^+-free membranes.

We were also interested in determining the quantity of NaCl present in PFSI films which had been equilibrated with 1 M NaCl. As we will see below, this is an important question; the excess NaCl acts as the supporting electrolyte and carries the migration current in the film during electrochemical experiments. To determine the NaCl concentration, the PFSI membranes were equilibrated with 1 M NaCl for three days. The membranes were weighed, dried and then reweighed; this yielded the equilibrium water contents for the NaCl-equilibrated membranes. The dried membranes were then stirred in pure water for 3 days, to remove the excess NaCl. The membranes were then redried and reweighed. The quantity of NaCl which had partitioned into the membranes was determined by difference.

The densities of the NaCl-equilibrated membranes were also determined. This was accomplished by measuring the dimensions of the NaCl-equilibrated membranes; these dimensions yielded the equilibrium film volume. The weight of the dry, NaCl-free membrane was then divided by this volume to yield the membrane density.

Results and Discussion

This Results and Discussion section is organized as follows: First, we demonstrate that the theoretical model (11,12), which was developed assuming semi-infinite diffusion in solution, is applicable to the polymer-coated

ultramicroelectrodes used here. We, then, show that the electrochemical determinations of D_{app} are not complicated by coupled diffusion and migration of the electroactive counterion. After this preliminary section, we discuss, in qualitative terms, the shapes of the cyclic voltammetric waves obtained at the film-coated ultramicroelectrodes.

The chronoamperometrically-determined D_{app}'s and C's for the electroactive cations, FA^+ and $Fe(bpy)_3^{2+}$, are then presented. These D_{app}'s and C's are then used to quantitatively analyze the voltammetric data. This is accomplished by using the chronoamperometrically-determined D_{app}'s and C's and the theory of Osteryoung et al. (23) to calculate voltammetric maximum currents for the film-coated ultramicroelectrodes. As we shall see, these calculated maximum currents agree with the experimental voltammetric currents.

We have found that D_{app} varies markedly with the concentration of electroactive cation present in the ionomer film. This concentration dependence is discussed, in detail, in the next section of the paper. D_{app} also varies with the equivalent weight of the Dow PFSI. This EW dependency is discussed in the penultimate section of this paper. Finally, we compare D_{app}'s for FA^+ in solution-processed Nafion with the corresponding D_{app}'s in recast Nafion.

Proof That the Chronoamperometric Theory (11,12) Applies - A number of preconditions must be met if the chronoamperometric theory discussed above is to be applied to the ionomer film-coated ultramicroelectrode. First, the diffusion layer of the electroactive cation must remain within the polymer film throughout the duration of the experiment. If the time, t, for the experiment is known, the diffusion layer thickness, δ, can be estimated via

(24)

$$\delta = (2D_{app}t)^{1/2} \quad (5)$$

The timescale for the experiment can be calculated using τ (Equation 2). The maximum value for τ in these experiments was 0.8. Solving Equation 2 for t and substituting t into Equation 5 gives $\delta = 3.4\ \mu m$.

The film thicknesses for the various membranes studied here were calculated from the amount of polymer applied to the electrode surface, the area of the electrode surface (Pt plus glass) and the density of the NaCl-equilibrated ionomer. The experimentally-determined densities and the calculated film thicknesses are shown in Table I. Because the film thicknesses are all greater than the diffusion layer thickness, the first precondition is satisfied.

It should be stressed, however, that film thickness does not enter into the determination of D_{app} and C in the chronoamperometric method described here. This represents a tremendous advantage over conventional, macro-sized electrode determinations of D_{app} and C where the film thickness must be known (7). Accurate thickness measurements are difficult to obtain for films coated onto an electrode surface since the thickness measurement, in many cases, must be made with the film-coated electrode removed from solution. Furthermore, changes in film thickness with electroactive cation loading and with oxidation or reduction of this ion are often ignored, leading to error in D_{app} determinations at conventional macro-sized electrodes (7).

The second important consideration for accurate D_{app} determinations at the ionomer film-coated ultramicroelectrode is coupled diffusion (9). Coupled diffusion is a phenomenon that occurs in permselective membranes

(9). Permselective membranes contain fixed charged sites (i.e. SO_3^- sites). To maintain electroneutrality, these membranes must also contain an equal number of ions of the opposite charge (counterions).

Now, consider a cation, FA^+, diffusing into an ionomer membrane in which the counterion is initially Na^+. In order to maintain electroneutrality, FA^+ can move into the membrane no faster than the rate at which Na^+ moves out of the membrane. As a result, FA^+ diffusion is "coupled" to Na^+ diffusion. The measured D_{app} is, therefore, a composite of the true diffusion coefficient for FA^+ (D_{FA+}) and the diffusion coefficient for Na^+ (D_{Na+}). Since D_{Na+} is much greater than D_{FA+} (6a,7d), coupled diffusion results in a measured D_{app} that is greater than the true D_{FA+} (9). Ideally, the electrochemical method should yield a D_{app} which is identical to D_{FA+}. This will only be true if coupled diffusion is eliminated.

In addition to coupled diffusion, migration can be a problem in electrochemical experiments in permselective media (9,25). Chronoamperometric theory assumes that the electroactive cation moves only by diffusion. However, if the membrane is permselective, there is no excess electrolyte to carry the migration current (9). Thus, unless the mobility or concentration of the electroactive cation is very low, the electroactive cation will carry some migration current. Since the theory used here does not account for migration of the electroactive cation, migration of this cation should be eliminated.

In this study, we circumvented the migration and coupled diffusion problems by using high supporting electrolyte and low electroactive cation concentrations. At high external electrolyte concentrations, Donnan exclusion breaks down and excess electrolyte partitions into the film (9).

When excess electrolyte is present, mobile co-ions (Cl^- in this case) are available to serve as the FA^+ counterions and coupled diffusion is eliminated (i.e. the situation becomes analogous to diffusion in solution containing supporting electrolyte).

To prove that excess electrolyte was present in these films, the NaCl concentrations in the films were determined gravimetrically. An average concentration of 1.0 M was obtained for films which had been equilibrated with 1 M NaCl. Note that this NaCl concentration is expressed in terms of the volume of water present in the film and not in terms of the total film volume. Since NaCl, and the electroactive counterions, reside primarily in the water-containing domains within Nafion (6c,26), the concentrations of these species are more accurately expressed on a per water volume, rather than a per film volume basis.

Excess electrolyte also solves the migration problem. The fraction of migration current carried by the electroactive cation (i.e. the transference number for this cation (24)) can be calculated as follows: The diffusion coefficients for Na^+ and Cl^- in Nafion membranes are 9×10^{-7} cm^2s^{-1} (6a) and 5×10^{-8} cm^2s^{-1} (6a), respectively. The concentration of electroactive cation loaded into the Nafion films ranged from 0.012 to 0.48 M (see Figures 6 and 7). Taking the highest concentration (0.48 M), the measured D_{app}, and the D's for Na^+ and Cl^-, a transference number for the electroactive cation in Nafion of 1.4×10^{-5} was calculated. Clearly, even in this worst case situation (highest concentration of electroactive cation), the migration current carried by the electroactive cation is essentially zero. Analogous conclusions were reached for the other PFSI's investigated here.

Qualitative Analyses of Cyclic Voltammograms for the Film-Confined Electroactive Cations. - The shape of the voltammogram at an ionomer film-coated ultramicroelectrode provides a qualitative indication of the magnitude of D_{app} for the electroactive cation in the ionomer film (23). Cyclic voltammograms (5 mVs^{-1}) for Nafion and Dow PFSI film-coated ultramicroelectrodes, containing two different concentrations of FA^+, are shown in Figures 3 and 4, respectively. The films in Figures 3a and 4a contain a low concentration of FA^+; whereas, the films in Figure 3b and 4b contain a higher concentration of FA^+.

The voltammograms in Figure 3a and 4a have a sigmoidal shape indicating the predominance of radial diffusion to the substrate electrode (12a,27). On the other hand, the voltammograms in Figure 3b and 4b are peak-shaped indicating predominately linear diffusion to the substrate electrode. These changes in the shapes of the voltammograms can be analyzed using Osteryoung's theory of voltammetry at ultramicroelectrodes (23).

Osteryoung investigated the effects of the electrode radius (r), the scan rate (ν), and the diffusion coefficient (D) on the shape of the voltammogram at an ultramicroelectrode. The effects of these factors can be accounted for through the dimensionless parameter, p, where (23)

$$p = (nFr^2\nu/RTD)^{1/2} \qquad (6)$$

When p is large, linear diffusion predominates, and the voltammogram is peak-shaped. Conversely, when p is small, radial diffusion predominates, and sigmoidal voltammograms are obtained (23).

The shapes of the voltammograms in Figures 3 and 4 clearly show that p is small when the concentration of electroactive cation in the film is low

and that p is large when the concentration of electroactive cation in the film is high. Note, however, that p should be independent of the concentration of the electroactive species (Equation 6). Furthermore, the electrode radii and the scan rates are the same for the voltammograms shown in Figures 3 and 4. Therefore, the only way to explain the observed changes in peak shape with concentration is to suggest that *D_{app} for FA^+ decreases dramatically with the quantity of FA^+ loaded into the film.* As we shall see, the chronoamperometric data presented below corroborate this conclusion.

Evaluation of D_{app} and C - A typical plot of i vs. $t^{-1/2}$ for a potential step at an FA^+-loaded, solution-processed Nafion film-coated ultramicroelectrode is shown in Figure 5. As theory predicts (Equation 1), this plot is linear (R^2 = 0.999). Using Equations 3 and 4, D_{app} and C can be determined from the slopes and intercepts of such plots; these data are shown in Table II. Analogous D_{app} and C data were obtained for FA^+ in recast Nafion film (Table III), for $Fe(bpy)_3^{2+}$ in solution-processed Nafion film (Table IV), and for FA^+ in solution-processed Dow 803 EW (Table V), Dow 909 EW (Table VI), and Dow 1076 EW (Table VII) films.

In agreement with the cyclic voltammetric data, Table II through VII show that D_{app} varies inversely with C. The effect of C on D_{app} can be illustrated more graphically by plotting D_{app} as a function of C (Figures 6, 7 and 8). These plots show that the most pronounced change in D_{app} occurs over a very narrow range in C (ca. zero to 1 x 10^{-4} moles cm^{-3}). D_{app} drops by ca. one and a half orders of magnitude over this narrow concentration range. The reasons for this dramatic decrease in D_{app} will be discussed in a later section of this paper.

Quantitative Analysis of the Voltammetric Data - Osteryoung et al. have derived the following expression which can be used to calculate the maximum current, i_m, for a linear sweep voltammogram at an ultramicroelectrode (23)

$$i_m = 4nFrDC[0.34\exp(-0.66p)+0.66-0.13\exp(-11/p)+0.351p] \quad (7)$$

Equation 7 was used to calculate theoretical maximum currents for FA^+ voltammograms at the solution-processed Nafion film-coated ultramicroelectrodes. The chronoamperometrically-determined D_{app}'s and C's for FA^+ (Table II), the experimentally determined r, and the experimental scan rate (5 mVs^{-1}, Figure 3) were used in these calculations.

The calculated and experimental (28) maximum currents are compared in Table VIII. The calculated currents differ by no more than 5 percent from the corresponding experimental values; this excellent agreement allows us to draw a number of important conclusions. First, the data in Table VIII indicate that the theory of Osteryoung et al. (12) applies not only to diffusion in solution but to diffusion in polymer films. Second, the fact that the chronoamperometric results fit this purely diffusional model provides compelling evidence that migration of the electroactive cation is, indeed, insignificant.

Finally, it is important to note that cyclic voltammograms for electroactive cations in thick Nafion films coated onto macro-sized electrode surfaces are strongly distorted by resistive effects (7d,8). Because of this distortion, cyclic voltammetric data at macro-sized film-coated electrodes are rarely used to obtain D_{app} or other quantitative data. The agreement between the chronoamperometric and voltammetric data observed here indicates that simple voltammetric experiments could be used to obtain

Dapp's and other parameters (e.g. heterogeneous rate constants) at film-coated ultramicroelectrodes (15,29). This important advantage accrues because the ultramicroelectrode draws substantially lower currents, and is thus less susceptible to resistive distortion.

Why does D_{app} Vary with C? - A number of other researchers have observed concentration-dependent D_{app}'s in Nafion (see e.g. 7e,f,g). A variety of explanations have been proposed to explain this concentration dependency; we briefly review these proposed explanations, below, and show that none can be applied to the data reported here. Note, however, that the PFSI films studied here contained lower concentrations of electroactive cations than films used in the previous investigations. Thus, the discussion presented below should not be construed a indicating that the prior analyses of electrochemical transport data in PFSI's is incorrect.

Anson et al. have previously reported concentration-dependent D_{app}'s for electroactive cations in Nafion films on electrode surfaces (7e,f,g). In this section, we discuss the various proposed explanations for this concentration dependence, and attempt to identify the genesis of the concentration dependence observed here. However, because the effect of concentration on D_{app} should, in principle, be dependent on the mechanism of charge transport (7a,b,e,f,g), we first briefly review the proposed mechanisms by which charge may be transported through polymer films on electrode surfaces (7,30).

Charge may be transported across an electronically insulating polymer film by either ionic diffusion or electron hopping (7a,b). Ionic or "true" diffusion involves the physical movement of the electroactive species through the polymer matrix. Electron hopping, on the other hand, refers to

charge propagation via the self-exchange of electrons between oxidized and reduced sites within the polymer film (i.e. redox conduction (31)).

The mechanism of charge-transport for electroactive cations loaded into Nafion films on electrode surfaces has been the subject of a number of previous investigations (7). These studies suggest that charge-transport for FA^+ occurs predominately by ionic diffusion (7b,d). In contrast, prior analyses suggest that charge-transport for $Fe(bpy)_3^{2+}$ occurs predominately by electron hopping (7d).

Considering the proposed ionic diffuser first, note that prior investigations have yielded D_{app}'s that decrease with increasing concentration of diffusing ion (7e,f,g). A variety of explanations have been (or could be) proposed to explain this concentration dependency; these include, concentration induced changes in film water content (32), electrostatic cross-linking (7g), location of the diffuser within the complicated microdomain structure of Nafion (7e), and single file diffusion (7e,f). The relevance of each of these proposed explanations to the data obtained here is discussed below.

We first explore the possibility that changes in film water content (induced by the incorporation of the hydrophobic electroactive cation (21)) are responsible for the concentration-dependent D_{app}'s. If the water content is sufficiently low, contact ion pairs could form between the diffusing cation and the fixed anionic sites in the film; ion pair formation would clearly lower the mobility of the diffusing cation (26).

Figure 9 shows that the equilibrium water content of the Nafion membrane drops when FA^+ is ion-exchanged into the membrane. Similar decreases in equilibrium water contents have been observed when other hydrophobic cations

have been partitioned into Nafion (21). As indicated in Figure 9, the water content decreases from approximately 21 percent, for an unloaded Nafion film, to ca. 18 percent when C_{FA+} reaches the maximum value employed in the electrochemical investigations described here (Figure 6).

Is this decrease from 21 to 18 percent water sufficient to promote ion pair formation between the diffusing FA^+'s and the immobile $-SO_3^-$ sites? In terms of water molecules per $-SO_3^-$ site, this drop in water content corresponds to a change from ca. 12 waters per $-SO_3^-$ site to ca. 11 waters per $-SO_3^-$ site (33). This change is clearly insignificant. Furthermore, infrared spectroscopic studies have shown that ion pairing does not become significant until the membrane water contents drop below 7 percent (26). Thus, the decrease in D_{app} with the concentration of the electroactive counterion cannot be attributed to changes in the water content of the film.

Electrostatic cross-linking has previously been invoked to explain concentration-dependent diffusion coefficients in ion-exchange polymer films on electrode surfaces (7g). Note, however, that FA^+ is monovalent and thus should not promote electrostatic cross-linking. Furthermore, the largest drop in D_{app} occurs at very low concentrations of the electroactive cation, where the effects of electrostatic cross-linking should be minimal. Thus, the concentration-dependent D_{app}'s observed here cannot be blamed on electrostatic cross-linking.

The Nafion and Dow polymers apparently have very complex microdomain structures (1,6c,19). One of the most popular models for this microstructure assumes that Nafion is triphasic. These phases are the ionic cluster phase, a teflon-like chain material phase, and an interphase which separates the ionic and chain material microphases (6c). According to this model, water

and SO_3^- sites reside in both the ionic and the interfacial regions. However, because the interfacial region contains higher concentrations of chain material, the interphase is more hydrophobic, and has a lower void volume, than the cluster phase (6c).

This three phase model has been used by Anson and by Yeager to explain concentration-dependent D_{app}'s in Nafion films (7e) and membranes (6c,d). The essence of these analyses is that cations which reside in the ionic cluster can diffuse faster than cations located in the lower void volume interphase (6c,7e). If this is true, than the concentration-dependent D_{app}'s observed in this investigation might be explained as follows. Assume that the first electroactive cations which enter the film (i.e. at low loading) preferentially reside in the cluster region. Because of the higher void volume, these "first-loaded" cations would diffuse at a higher rate than subsequently-loaded cations which must reside in the interfacial region. Thus, if this scenario is correct, the apparent diffusion coefficient would be expected to decrease as the concentration of electroactive cation in the film increases (Figure 6).

Unfortunately, this proposed explanation is completely at odds with prior spectroscopic analyses of Nafion (21). We have shown that at very low loadings, hydrophobic cations preferentially occupy the most hydrophobic sites in the film. When these sites are full, the subsequently-loaded cations are forced to occupy hydrophilic sites in the membrane. If the three phase formalism of Yeager et al. is correct, these data would suggest that D_{app} would increase (not decrease) with loading. Clearly, the three phase morphological model cannot be invoked to explain the concentration dependency observed here.

Finally, Anson has suggested that "single file diffusion" (7e) might cause D_{app}'s for electroactive cations in Nafion to decrease with concentration. In the classical sense (7e,34), single file diffusion refers to a transport mechanism in which a cation moves through a membrane by hopping between fixed anionic sites. If the concentration of the diffusing cation in the membrane is high, the rate of transport can become limited by the availability of free anionic sites; i.e. transport is impeded by the requirement that the cations diffuse "single file" past the few available sites.

The single file diffusion model predicts that the apparent diffusion coefficient will decrease as the concentration of diffusing species increases (7e). While this is in apparent agreement with the experimental data (Figures 6 and 8), a more careful analysis indicates that single file diffusion (in the classical sense) is not responsible for the diminution in D_{app} observed here. Note, first, that the largest drop in D_{app} occurs over a concentration region where less that 2 percent of the $-SO_3^-$ sites are occupied by the diffusing cation. The effects of single file diffusion should not be manifested in this low concentration region where over 98 percent of the fixed sites are available for electroactive cation transport. Thus, while the single file diffusion model is in qualitative agreement with the experimental data, there is significant quantitative disagreement.

Furthermore, and perhaps more importantly, the large excess of free supporting electrolyte in these films means that the single file diffusion model (in the classical electrostatic sense) cannot be operative. This free supporting electrolyte ensures that an ample supply of mobile anions is available to accompany the electroactive cations as they diffuse through the

film. Thus, the electroactive cations do not have to wait in a queue for the next fixed anionic site to become available.

We propose that an alternative (nonelectrostatic) form of single file diffusion accounts for the concentration-dependent Dapp's observed here. Again, this proposed explanation applies only to the low loading-level case investigated here. This nonelectrostatic single file diffusion is similar to the "pore diffusion" effect discussed by Heckmann (35). Gierke has suggested that the ionic clusters in Nafion are connected by narrow (ca. 10 A diameter) channels (36-38). Our recent investigations suggest that this cluster-channel model is also applicable to the Dow PFSI's (19). Because the channels present in these polymers have diameters which are approximately the same size as the diameters of the electroactive cations (36), the rate of diffusion in the channel is lower than in the cluster (38).

When the concentration of electroactive cation is increased, this restricted channel diffusion will create a "bottleneck" at the mouth of the channel. To understand this bottleneck effect, consider an FA^+ ion (labeled FA^+_1) which is diffusing from cluster A to cluster B through a narrow interconnecting channel. If no other FA^+ molecules are present, FA^+_1 diffuses rapidly to the channel, slows down as it traverses the channel and then diffuses rapidly through the next cluster.

Now assume that two other FA^+'s (FA^+_2 and FA^+_3) are also attempting to traverse the channel at the same time as FA^+_1. In this case, the rate of transport of FA^+_1 is retarded as it waits for FA^+_2 and FA^+_3 to clear the channel. Thus, slow channel diffusion causes the apparent diffusion coefficient to decrease with increasing concentration of diffusing ion (35).

The channel bottleneck model proposed above is more consistent with the

experimental data than the electrostatic single file diffusion model. Note that D_{app} for FA^+ decreases at about the 2 percent loading level. Assuming that the number of SO_3^- sites per cluster is ca. 80 (as calculated for a Na^+-form, 1150 EW membrane with a 20 percent water content (39)), 2 percent SO_3^- sites occupied corresponds to about 1.7 FA^+ molecules per cluster. Thus, in agreement with the bottleneck theory, the rate of diffusion in Nafion is fastest when the average number of electroactive cations per cluster is less than 1 and decreases sharply when the average number per cluster becomes greater than one.

Note further that D_{app}'s for FA^+ in the Dow polymers (Figure 8) decrease over the same concentration range as is observed in the Nafion polymers (Figures 6 and 7). Again, the conventional electrostatic single file diffusion model cannot account for this dramatic drop in D_{app} (vide supra). Thus, we propose that the decrease in D_{app} with increasing C observed in the Dow PFSI's is also caused by the bottleneck effect.

The bottleneck theory proposed above seems reasonable when charge transport in the polymer film occurs via true ionic diffusion. However, let us now turn our attention to the suspected electron hopping diffuser, $Fe(bpy)_3^{2+}$. The Dahms-Ruff theory for electron hopping diffusion predicts that D_{app} should <u>increase</u> with concentration (7a,b,e); this is diametrically opposed to the observed experimental trend (Figure 7).

The magnitudes of the apparent diffusion coefficients also seem to be at odds with the electron hopping model. According to the Dahms-Ruff model, the measured apparent diffusion coefficient is the sum of an electron hopping diffusion coefficient and the true ionic diffusion coefficient; the electron hopping diffusion coefficient makes an appreciable contribution to

the sum only when the true ionic diffusion coefficient is small (7a,b,e). For this reason, apparent diffusion coefficients which are dominated by electron hopping are always very small (ca. 10^{-10} cm^2s^{-1}). Note, however, that at low concentrations, D_{app} for $Fe(bpy)_3^{2+}$ is ca. 10^{-8} cm^2s^{-1} (Figure 7); this relatively large value suggests that this is not an electron hopping D_{app}.

The bottleneck diffusion model, described above, can be used to explain these apparent contradictions between the experimental data and the predictions of the electron hopping model. The key point is that electron hopping will make a significant contribution to charge-transport only when ionic diffusion is slow. However, according to the bottleneck model, ionic diffusion at low concentrations is very fast. The obvious conclusion is that at the lowest concentrations investigated here, the ionic diffusion coefficient for $Fe(bpy)_3^{2+}$ is so high that electron hopping does not make an appreciable contribution to the measured apparent diffusion coefficient.

Thus, we propose that, at low loading levels, $Fe(bpy)_3^{2+}$ transports charge by true ionic diffusion. This explains why the apparent diffusion coefficients at low concentrations are much higher than is expected for an electron hopper and why, in disagreement with the electron hopping model, D_{app} decreases as the concentration of $Fe(bpy)_3^{2+}$ increases. As the concentration increases, the bottleneck effect causes $Fe(bpy)_3^{2+}$'s ionic diffusion coefficient to drop (Figure 7), just as FA^+'s D_{app} drops (Figure 6). This explains why the D_{app}'s for FA^+ (a known ionic diffuser (7b,d)) and $Fe(bpy)_3^{2+}$ show identical concentration dependencies.

It seems likely that ultimately the true ionic diffusion coefficient for $Fe(bpy)_3^{2+}$ would drop to the point that electron hopping would become

significant. However, the concentration range employed here is probably not, yet, high enough to support appreciable rates of electron hopping diffusion. Furthermore, as originally pointed out by Anson, the opposing effects of single file diffusion and electron hopping may mask the anticipated electron hopping-based increase in D_{app} with concentration (7g).

Finally, note that the break in the D_{app} vs. C curve for $Fe(bpy)_3^{2+}$ (Figure 7) occurs at approximately the same concentration as the break in the D_{app} vs. C curve for FA^+ (Figure 6). If the decrease in D_{app} with increasing C were electrostatic in origin, this break would occur over a lower concentration range for the divalent ion than for the monovalent ion. The fact that the experimental breaks occur at approximately the same concentration provides further evidence that the electrostatic single file diffusion model is not correct.

The question now becomes - why haven't previous investigations (including investigations from this laboratory (7d)) yielded data analogous to the results reported here. There are several reasons: first, the electroactive cation loading levels used here are <u>much lower</u> than loading levels used in most of the previous investigations. As indicated in the above discussion, many of the effects observed here are unique to the very low concentration range employed.

Second, we use ultramicroelectrodes; whereas, all previous investigations employed conventional macro-sized electrodes (7). As noted above, this is an important difference because ultramicroelectrodes draw significantly lower currents than macro-sized electrodes. As a result, the ultramicroelectrode data is more distortion-free than the macro-sized electrode data. Finally, as was clearly pointed out by Elliott, previous

investigations (including our own (7d)) made no effort to eliminate the effects of migration and coupled diffusion (9). In the current investigation, we have worked very hard to eliminate these problems. The previously reported results could be tainted by these effects.

Effect of Equivalent Weight on Diffusion in the Dow PFSI's - Figure 8 compares D_{app}'s for the various EW's of the Dow PFSI's. At all concentrations, the D_{app}'s for the 803 EW polymer are greater than the D_{app}'s for the 909 and the 1076 EW polymers. We have recently conducted an extensive investigation of the morphologies of the Dow PFSI's (19). These studies showed that while the 1076 and 909 EW polymers are partially crystalline, the 803 polymer is almost completely noncrystalline (19). It seems likely that this lack of crystallinity accounts for the higher mass-transport rates in the 803 EW polymer.

Diffusion in Solution-Processed vs. Recast Nafion Films - In a previous report from this laboratory, we discussed the chemical and morphological difference between solution-processed and recast Nafion (18). We found that the morphology of the solution-processed material is essentially identical to the morphology of as-received Nafion membrane (18). While the recast material has a similar morphology, the degree of microphase separation is less than in the solution-processed or as-received polymers (18).

In this final section of this paper, transport in solution-processed Nafion (17) is compared to transport in the recast material. The objective of this comparison is to see if the subtle differences in microstructure between these two forms of the polymer are reflected in the transport data. As far as we know, this is the first quantitative evaluation of ionic transport in the solution-processed material.

Figure 6 shows plots of D_{app} vs. loading level for FA^+ in both solution-processed and recast Nafion. Note that above ca. 3 percent SO_3^- sites occupied by FA^+, the diffusion coefficients in solution-processed and recast Nafion are identical. This result is not surprising; recall that at these higher loading levels, diffusion is limited by the bottleneck effect and not by the actual cluster or channel transport event.

At lower concentrations, however, transport is limited by diffusion within the channels that interconnect the ionic clusters. If the channels in the recast and solution-processed materials are not the same, the differences should be reflected in this low loading level transport data. In agreement with this analysis, note that at low concentrations, D_{app}'s in the recast material are lower than D_{app}'s in the solution-processed material.

These diffusion data appear to corroborate the conclusion reached from our prior investigations of the morphology of the recast polymer. The lower degree of microphase separation in the recast material (vide supra and (18)), causes the channels between the clusters to be more occluded with polymer chain material; this, in turn, results in a lower rate of transport.

Conclusions

We have shown here that chronoamperometry at polymer film-coated ultramicroelectrodes is a very powerful and convenient method for simultaneous determinations of D_{app}'s and C's of electroactive species loaded into polymer films. This approach offers unique advantages over the more conventional methods which use macro-sized electrodes (7). These advantages include - 1. At the ultramicroelectrode, D_{app} and C can be

determined from a single experiment. Two experiments are required to determine D_{app} and C at a macro-sized electrode. 2. Because an independent determination of C is not required, determinations of D_{app} are enormously simplified relative to determinations of D at a macro-sized electrode. 3. As was clearly demonstrated here, iR distortion is essentially negligible at the ultramicroelectrode. 4. The thickness of the film on the electrode surface does not need to be known in the ultramicroelectrode experiment.

Another interesting feature of the ultramicroelectrode experiment, which was not exploited here, is that this experiment can be conducted in the absence of any external electrolyte phase. Resistive effects would make this solid state electrochemical experiment impossible at a macro-sized electrode. Such solid state experiments have recently been described by Murray et al. (40) and by this laboratory (41).

This ultramicroelectrode experiment has allowed us to take a fresh look at the mechanism and rate of charge-transport in ionomers. This fresh look has provided new insight into the mechanism of the charge-transport process in these polymers and has shown that the rates of charge-transport (at low concentrations) can be much faster than previously expected. Perhaps more importantly, we have found that at low concentrations of electroactive cation in the film, charge-transport occurs purely by ionic diffusion rather than by electron self-exchange. While this conclusion is in qualitative agreement with the predictions of the relevant theoretical analysis (Dahms-Ruff), pure ionic diffusion D_{app}'s for $Fe(bpy)_3^{2+}$ have not been observed in previous investigations. As discussed in detail above, pure ionic diffusion predominates here because of the very low concentration range employed; previous investigators, in general, used much higher concentrations of

electroactive cation in the film.

Finally, this paper compares D_{app} data for a number of PFSI's, varying in EW, and chemical and morphological structure. Previous electrochemical analyses of this type have focused on only two EW's of the Nafion PFSI. The most interesting aspect of this comparison is the remarkable similarity in the effect of concentration of electroactive cation on the experimentally-determined D_{app}'s (Figures 6 and 8). All of the polymers studied here share a common morphological feature, ionic clusters. We have interpreted the D_{app} data obtained in terms of a very simple model which takes into account the effect of the cluster on the rate of transport in these polymers.

TABLE I. Densities and Thicknesses for Ionomer Films Equilibrated in 1 M NaCl.

ionomer	EW	density (g/cm^3)	film thickness (μm)
Nafion	1100	1.35	10.4
Dow	803	1.30	11.7
Dow	909	1.45	10.5
Dow	1076	1.66	9.2

TABLE II: Chronoamperometrically-Determined D's and C's for FA^+ in Solution-Processed Nafion Films.

C (moles/cm^3) x 10^4	D (cm^2/s) x 10^{10}
0.12	110
0.23	91
0.49	28
1.0	8.7
1.9	3.6
2.2	3.0
2.3	3.6
2.7	3.3
2.9	2.4
3.0	2.2
4.3	0.66

TABLE III: Chronoamperometrically-Determined D's and C's for FA^+ in Recast Nafion Films.

C (moles/cm^3) x 10^4	D (cm^2/s) x 10^{10}
0.13	62
0.34	28
0.43	27
0.58	12
1.5	5.4
2.1	2.2
2.6	2.3
3.0	2.2
3.1	2.4
4.3	0.47

TABLE IV: Chronoamperometrically-Determined D's and C's for $Fe(bpy)_3^{2+}$ in Solution-Processed Nafion Films.

C (moles/cm^3) x 10^4	D (cm^2/s) x 10^{10}
0.24	59
0.51	17
1.1	7.1
1.9	2.5
2.0	2.2
2.1	2.2
2.8	1.6
3.8	0.25

TABLE V: Chronoamperometrically-Determined D_{app}'s and C's for FA^+ in Solution-Processed 803 EW Dow PFSI Films.

C (moles/cm^3) x 10^4	D_{app} (cm^2/s) x 10^{10}
0.057	91
0.16	82
0.91	28
1.5	19
1.6	15
1.7	14
2.0	14

TABLE VI: Chronoamperometrically-Determined D_{app}'s and C's for FA^+ in Solution-Processed 909 EW Dow PFSI Films.

C (moles/cm^3) x 10^4	D_{app} (cm^2/s) x 10^{10}
0.064	70
0.11	44
0.44	17
0.53	20
1.0	7.8
1.2	7.3
1.3	6.5
1.9	6.9

TABLE VII: Chronoamperometrically-Determined D_{app}'s and C's for FA^+ in Solution-Processed 1076 EW Dow PFSI Films.

C (moles/cm^3) x 10^4	D_{app} (cm^2/s) x 10^{10}
0.44	17
0.53	20
1.6	4.2
1.7	3.0
2.5	2.1
3.3	2.8
3.9	1.9

TABLE VIII: Comparison of Experimental and Theoretical Voltammetric Maximum Currents for FA^+ in Solution-Processed Nafion Films.

C[a] (moles/cm^3) x 10^4	D_{app}[a] (cm^2/s) x 10^{10}	Voltammetric Maximum Current	
		Experimental[b]	Theoretical[c]
0.12	110	36	36
0.49	28	62	64
1.9	3.6	28	26
2.7	3.3	95	98
2.9	2.4	69	72
4.3	0.66	55	57

a. C's and D_{app}'s for FA^+ in the film were determined chronoamperometrically.

b. Measured from cyclic voltammograms (e.g., Figure 3).

c. Calculated from Equations 6 and 7 using D_{app}'s and C's shown.

REFERENCES

(1) Eisenberg, A., Yeager, H.L., Eds. *Perfluorinated Ionomer Membranes*; American Chemical Society: Washington, DC, 1982; ACS Symp. Ser. No. 180.

(2) Grot, W. *Chem.-Ing.-Tech.* **1978**, *50*, 299.

(3) LaConti, A.B.; Fragala, A.R.; Boyack, J.R. *Proc.-Electrochem. Soc.* **1977**, *77-6*, 354.

(4) (a) Will,F.G. *J. Electrochem. Soc.* **1979**, *126*, 35. (b) Yeo, R.S.; Chin, D.-T. *J. Electrochem. Soc.* **1980**, *127*, 549.

(5) Yeo, R.S.; McBreen, J.; Kissel, G.; Kulesa, F.; Srinivasan, S. *J. Appl. Electrochem.* **1980**, *10*, 741.

(6) (a) Yeager, H.L.; Kipling, B. *J. Phys. Chem.* **1979**, *83*, 1836. (b) Yeager, H.L.; Kipling, B.; Dotson, R.L. *J. Electrochem. Soc.* **1980**, *127*, 303. (c) Yeager, H.L.; Steck, A. *J. Electrochem. Soc.* **1981**, *128*, 1880. (d) Herrara, A.; Yeager, H.L. *J. Electrochem. Soc.* **1987**, *134*, 2446.

(7) (a) Buttry, D.A.; Anson, F.C. *J. Electroanal. Chem.* **1981**, *130*, 333. (b) White, H.S; Leddy, J.; Bard, A.J. *J. Am. Chem. Soc.* **1982**, *104*, 4811. (c) Martin, C.R.; Rubinstein, I.; Bard, A.J. *J. Am. Chem. Soc.* **1982**, *104*, 4817. (d) Martin, C.R.; Dollard, K.A. *J. Electroanal. Chem.* **1983**, *159*, 127. (e) Buttry, D.A.; Anson, F.C. *J. Am. Chem. Soc.* **1983**, *105*, 685. (f) Buttry, D.A.; Saveant, J.M.; Anson, F.C. *J. Phys. Chem.* **1984**, *88*, 3086. (g) Tsou, Y.-M.; Anson, F.C. *J. Phys. Chem.* **1985**, *89*, 3818.

(8) Madja, M.; Faulkner, L.R. *J. Electroanal. Chem.* **1984**, *169*, 77.

(9) Elliott, C.M.; Redepenning, J.G. *J. Electroanal. Chem.* **1984**, *181*, 137.

(10) Lawson, D.R.; Whiteley, L.D.; Martin, C.R.; Szentirmay, M.N.; Song,

J.I. *J. Electrochem. Soc.* **1988**, *135*, 2247.

(11) Winlove, C.P.; Parker, K.H.; Oxenham, R.K.C. *J. Electroanal. Chem.* **1984**, *170*, 293.

(12) (a) Aoki, K.; Osteryoung, J. *J. Electroanal. Chem.* **1981**, *122*, 19. (b) Hepel, T.; Plot, W.; Osteryoung, J. *J. Phy. Chem.* **1983**, *87*, 1278.

(13) Martin, C.R.; Rhoades, T.A.; Ferguson, J. *Anal Chem.* **1982**, *54*, 1639.

(14) Szentirmay, M.N.; Martin, C.R. *Anal. Chem.* **1984**, *56*, 1898.

(15) Howell, J.O.; Wightman, R.M. *Anal. Chem.* **1984**, *56*, 524.

(16) Aoki, K.; Osteryoung, J. *J. Electroanal. Chem.* **1981**, *125*, 315.

(17) Moore, III, R.B.; Martin, C.R. *Anal. Chem.* **1986**, *58*, 2569.

(18) Moore, III, R.B.; Martin, C.R. *Macromolecules* **1988**, *21*, 1334.

(19) Moore, III, R.B.; Martin, C.R. *Macromolecules*, submitted.

(20) Szentirmay, M.N.; Campbell, L.F.; Martin, C.R. *Anal. Chem.* **1986**, *58*, 661.

(21) Szentirmay, M.N.; Prieto, N.E.; Martin, C.R. *J. Phys. Chem.* **1985**, *89*, 3017.

(22) Steck, A.; Yeager, H.L. *Anal. Chem.* **1980**, *52*, 1215.

(23) Aoki, K.; Akimoto, K.; Tokuda, K.; Matsuda, H.; Osteryoung, J. *J. Electroanal. Chem.* **1984**, *17*, 219.

(24) Bard, A.J.; Faulkner, L.R. *Electrochemical Methods*, John Wiley and Sons: New York, 1980; Chapter 4.

(25) (a) Yap, W.T.; Durst, R.A.; Blubaugh, E.A.; Blubaugh, D.D. *J. Electroanal. Chem.* **1983**, *144*, 69. (b) Doblhofer, K.; Braun, H.; Lange, R. *J. Electroanal. Chem.* **1986**, *206*, 93.

(26) (a) Komorski, R.A.; Mauritz, K.A. *J. Am. Chem. Soc.* **1978**, *100*, 7487. (b) Mauritz, K.A.; Lowry, S.R. *Polym. Prepr.* **1978**, *19*, 336.

(27) (a) Saito, Y. *Rev. Polarogr.* **1968**, *15*, 178. (b) Shoup, A.; Szabo, A. *J.*

Electroanal. Chem. **1982**, *140*, 237.

(28) (a) Experimental peak currents were background corrected as described in ref. 24 and 28b. (b) Whiteley, L.D.; Martin C.R. *Anal. Chem.* **1987**, *59*, 1746.

(29) Wipf, D.O.; Kristensen, E.W.; Deakin, M.R.; Wightman, R.M. *Anal. Chem.* **1988**, *60*, 306.

(30) (a) Kaufman, F.B.; Engler, E.M. *J. Am. Chem. Soc.* **1979**, *101*, 547. (b) Oyama, N.; Anson, F.C. *J. Am. Chem. Soc.* **1979**, *101*, 3450. (c) Peerce, P.J.; Bard, A.J. *J. Electroanal. Chem.* **1980**, *114*, 89. (d) Daum, P.; Murray, R.W. *J. Electroanal. Chem.* **1979**, *103*, 289.

(31) Pickup, P.G.; Murray, R.W. *J. Am. Chem. Soc.* **1983**, *105*, 4510.

(32) Note that the effect of water on the diffusion coefficients of electroactive cations in Nafion is not usually examined because the water concentration is unknown. We determine the water contents of FA^+-loaded Nafion membranes in a separate experiment (see Experimental section).

(33) Assuming that the water content changes with FA^+ concentration as shown in Figure 9.

(34) Hodgkin, A.L.; Keynes, R.D. *J. Physiol. (London)* **1955**, *128*, 61.

(35) Heckmann, K. In *Biomembranes*; L.A. Manson, Ed.; Plenum Press: New York, 1972; Vol. 3, p 127.

(36) Hsu, W.Y.; Gierke, T.D. *J. Membr. Sci.* **1983**, *13*, 307.

(37) The 10 A diameter reported in reference (36) is an approximate value. Clearly, the exact diameter of the cluster will vary with solvation, thermal history, etc. However, the luminescence quenching results of Lee and Meisel (38) show that intracluster diffusion is faster than intercluster diffusion.

(38) Lee, P.C.; Meisel, D. *J. Am. Chem. Soc.* **1980**, *102*, 5477.

(39) Gierke, T.D.; Munn, G.E.; Wilson, F.C. *J. Polym. Sci., Polym. Phys. Ed.* **1981**, 19, 1687.

(40) (a) Jernigan, J.C.; Chidsey, C.E.D.; Murray, R.W. *J. Am. Chem. Soc.* **1985**, *107*, 2824. (b) Reed, R.A.; Geng, L.; Murray, R.W. *J. Electroanal. Chem.* **1986**, *208*, 185. (c) Geng, L.; Reed, R.A.; Longmire, M.; Murray, R.W. *J. Phys. Chem.* **1987**, *91*, 2908.

(41) Whiteley, L.D.; Martin, C.R. *Pitts. Conf. Abs. No. 176*, **1986**.

ACKNOWLEDGEMENT

This work was supported by the Office of Naval Research, the Air Force Office of Scientific Research, and the Robert A. Welsh Foundation.

Figure Captions

Figure 1. The structure of duPont's Nafion (I) and Dow Chemical Company's PFSI (II).

Figure 2. Schematic diagram of the instrumental set-up for measuring very small currents at ultramicroelectrodes.

Figure 3. Cyclic voltammograms of FA^+ at solution-processed Nafion film-coated ultramicroelectrodes. The films contain (A) 1.2×10^{-5} and (B) 2.7×10^{-4} moles cm^{-3} FA^+. The scan rate was 5 mV s^{-1}.

Figure 4. Cyclic voltammograms of FA^+ at solution-processed (A) 803 EW Dow PFSI film containing 1.6×10^{-5} moles cm^{-3} FA^+ and (B) 1076 EW Dow PFSI containing 3.9×10^{-4} moles cm^{-3} FA^+. The scan rate was 5 mV s^{-1}.

Figure 5. Typical plot of current vs. $t^{-1/2}$ for a potential step from +0.25 to +0.55 V (vs. SCE) at an FA^+-loaded, solution-processed Nafion film-coated ultramicroelectrode.

Figure 6. Plots of D_{app} vs. concentration (or percent SO_3^- sites occupied) for FA^+-loaded, (o) solution-processed or (Δ) recast Nafion film-coated ultramicroelectrodes.

Figure 7. Plot of D_{app} vs. concentration for $Fe(bpy)_3^{2+}$-loaded, solution-processed Nafion film-coated ultramicroelectrodes.

Figure 8. Plots of D_{app} vs. concentration for FA^+-loaded, solution-processed (o) 803, (Δ) 909, and (□)1076 EW Dow PFSI film-coated ultramicroelectrodes.

Figure 9. Plot of percent water uptake vs. concentration of FA^+ in the Nafion membranes.

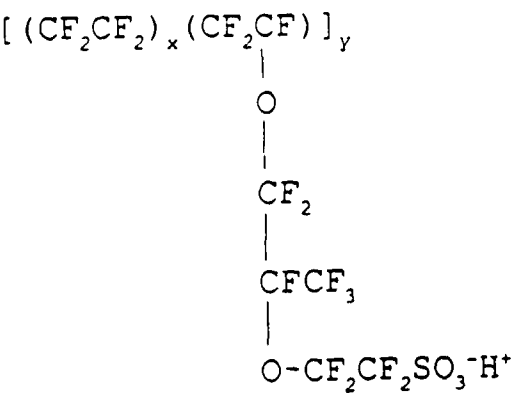

(I)

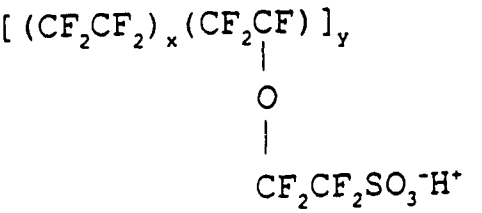

(II)

FIGURE 1

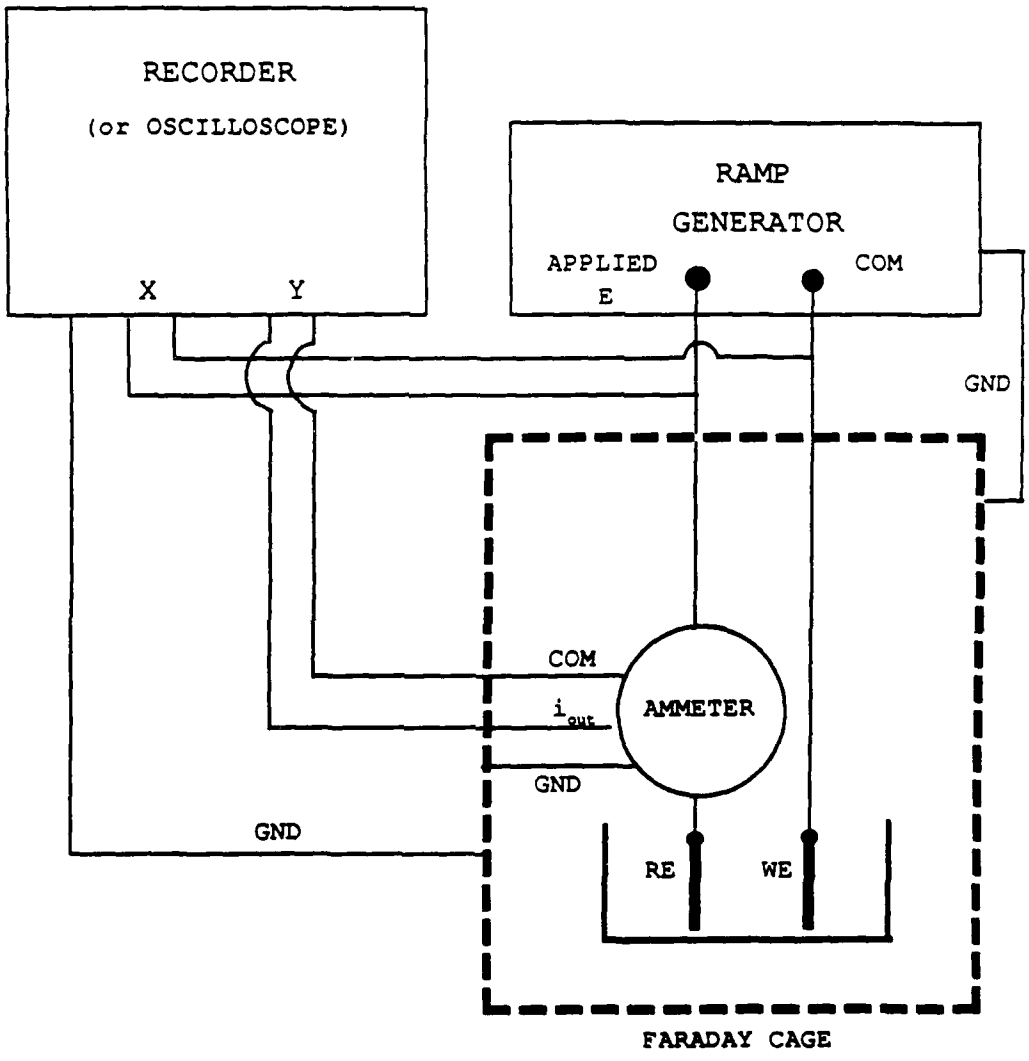
RECORDER
(or OSCILLOSCOPE)
X
Y
RAMP
GENERATOR
APPLIED
E
COM
GND
COM
i_{out}
AMMETER
GND
GND
RE
WE
FARADAY CAGE

FIGURE 2

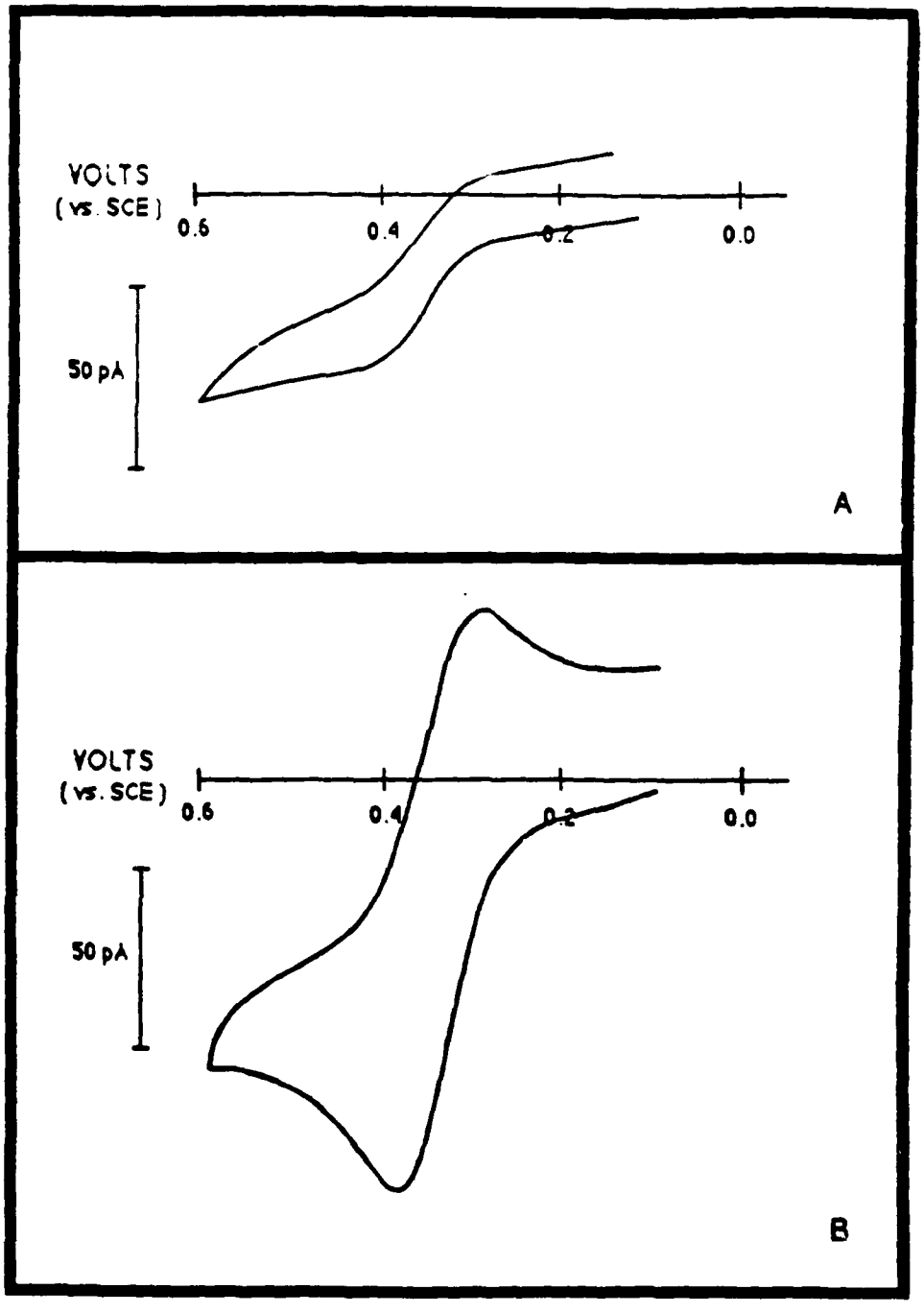

FIGURE 3

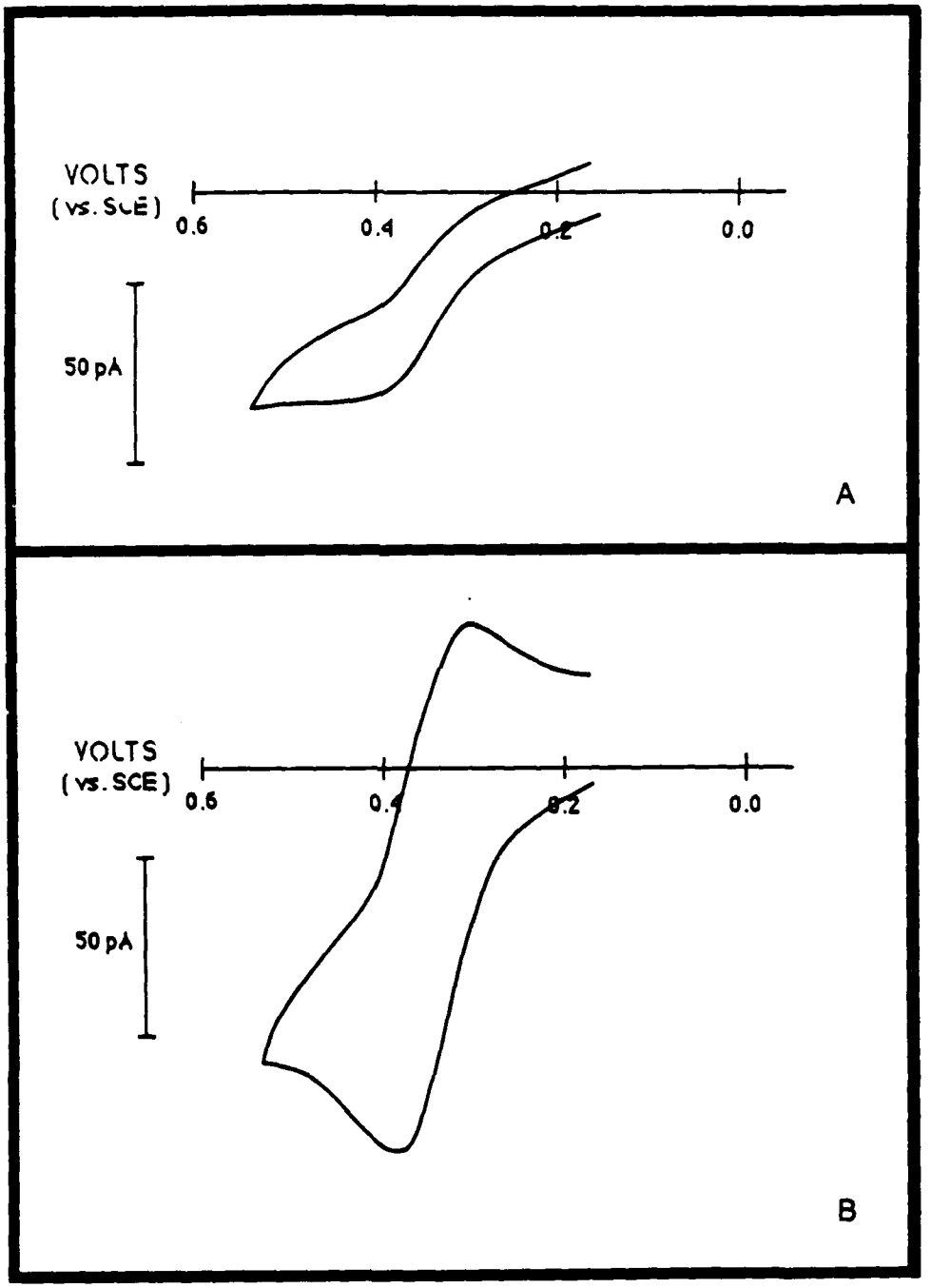

FIGURE 4

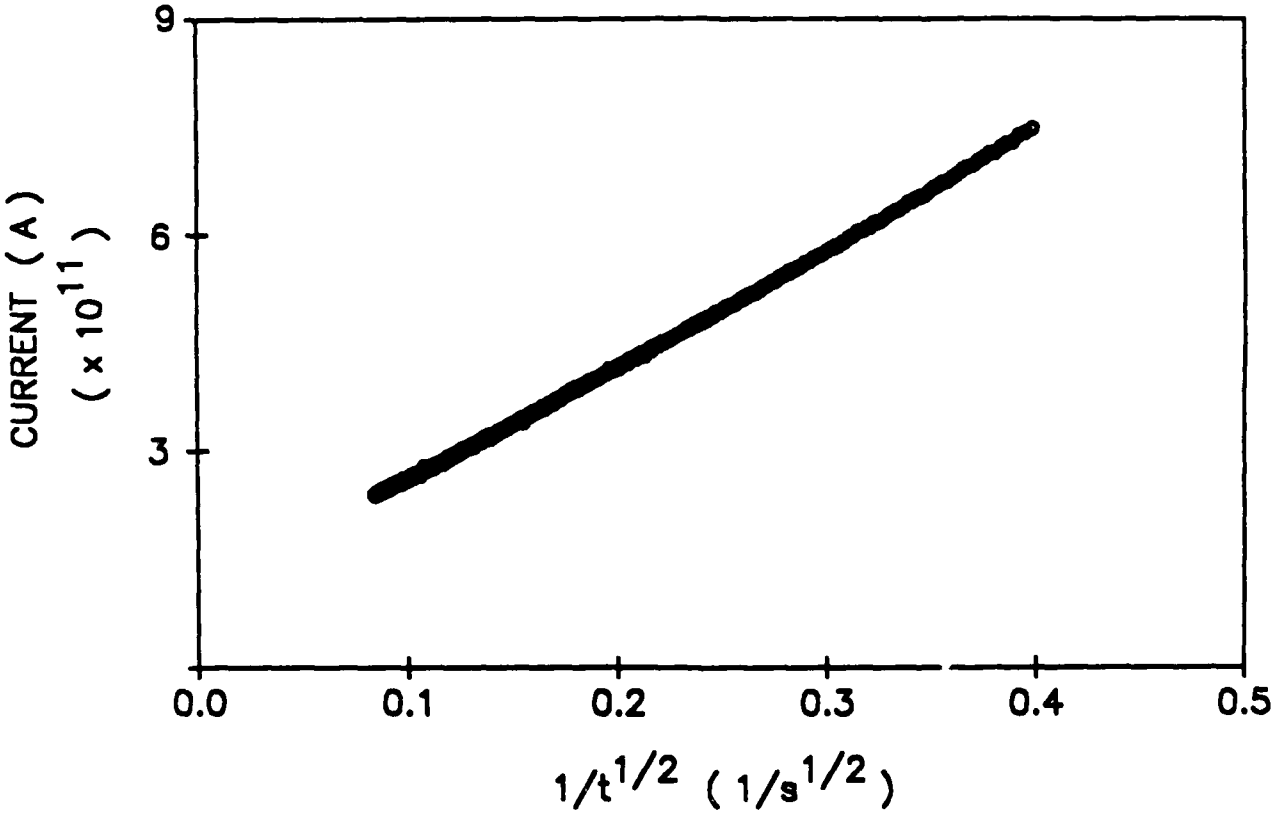

FIGURE 5

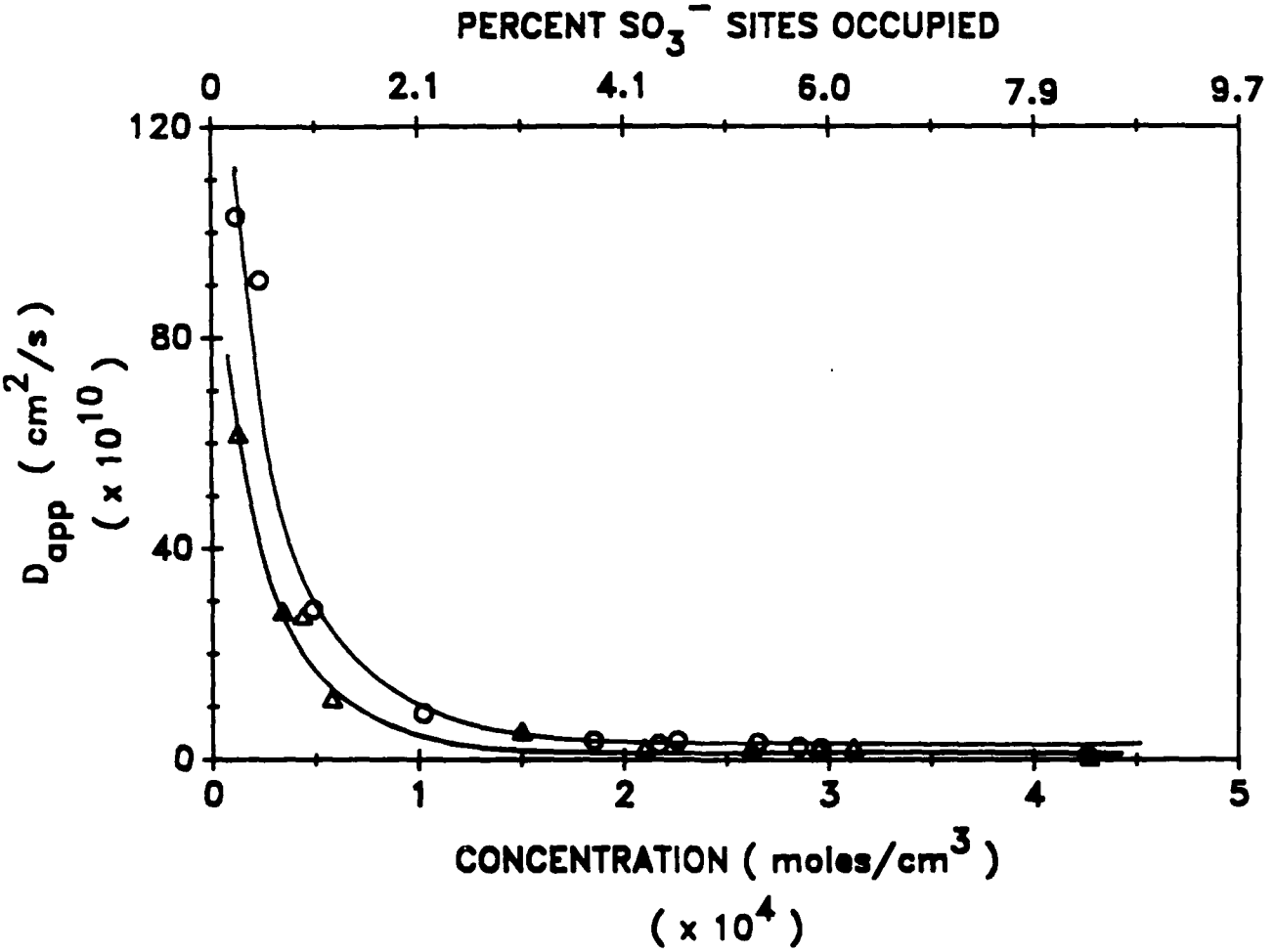
PERCENT SO_3^- SITES OCCUPIED
0
2.1
4.1
6.0
7.9
9.7
120
80
40
0
D_{app} (cm^2/s)
($\times 10^{10}$)
0
1
2
3
4
5
CONCENTRATION (moles/cm^3)
($\times 10^4$)

FIGURE 6

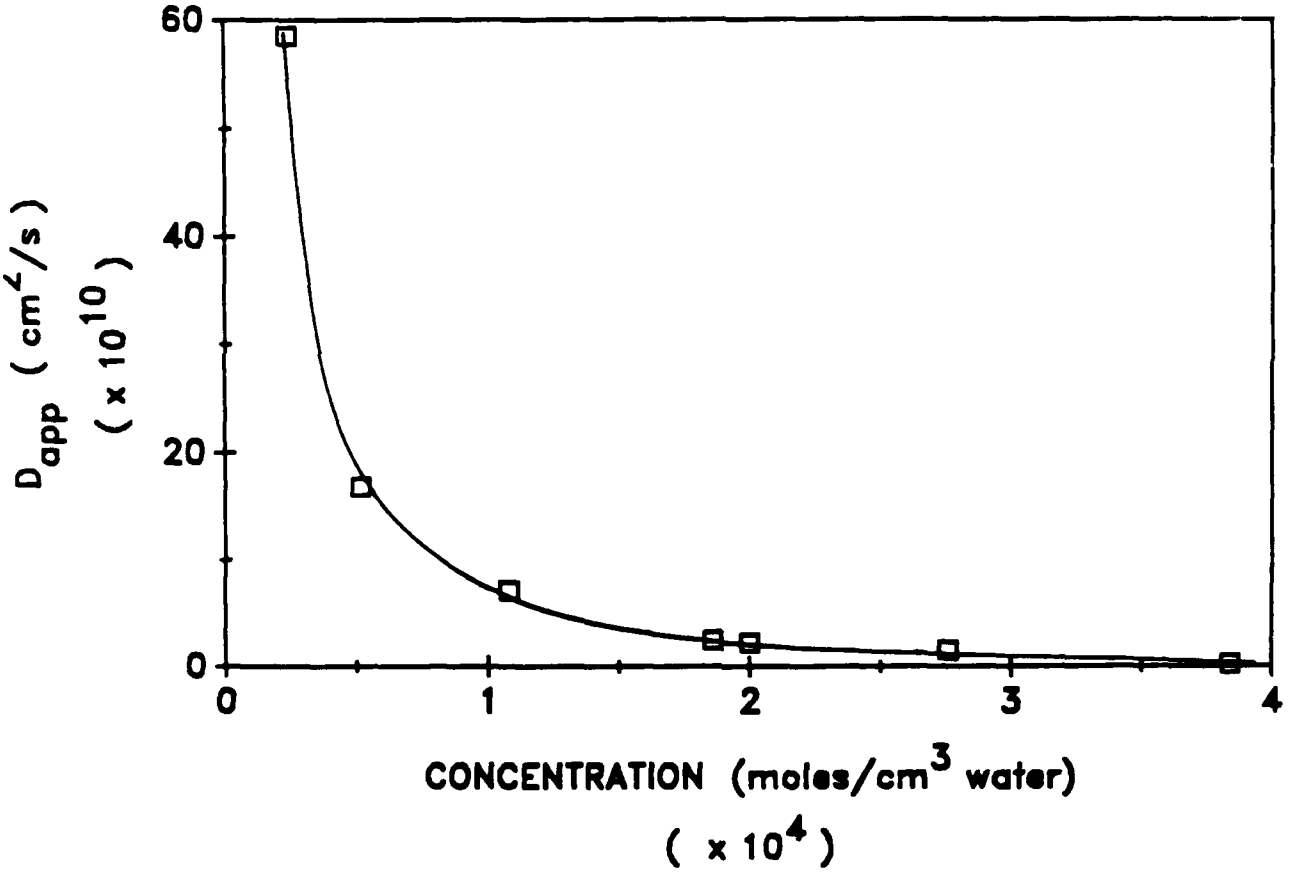
60
40
20
0
0
1
2
3
4
D_{app} (cm^2/s)
($\times 10^{10}$)
CONCENTRATION (moles/cm^3 water)
($\times 10^4$)

FIGURE 7

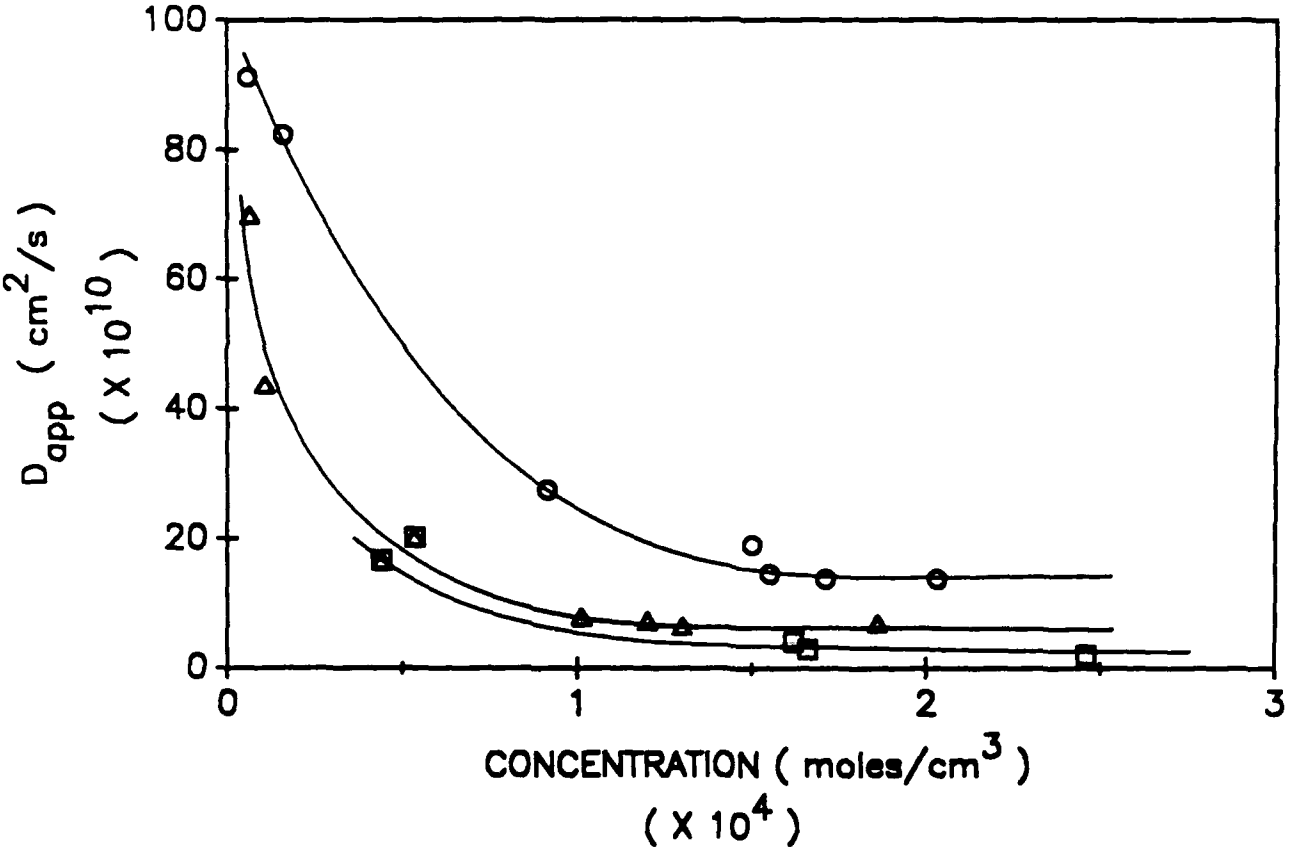
100
80
60
40
20
0
0
1
2
3
D_{app} (cm^2/s)
(X 10^{10})
CONCENTRATION (moles/cm^3)
(X 10^4)

FIGURE 8

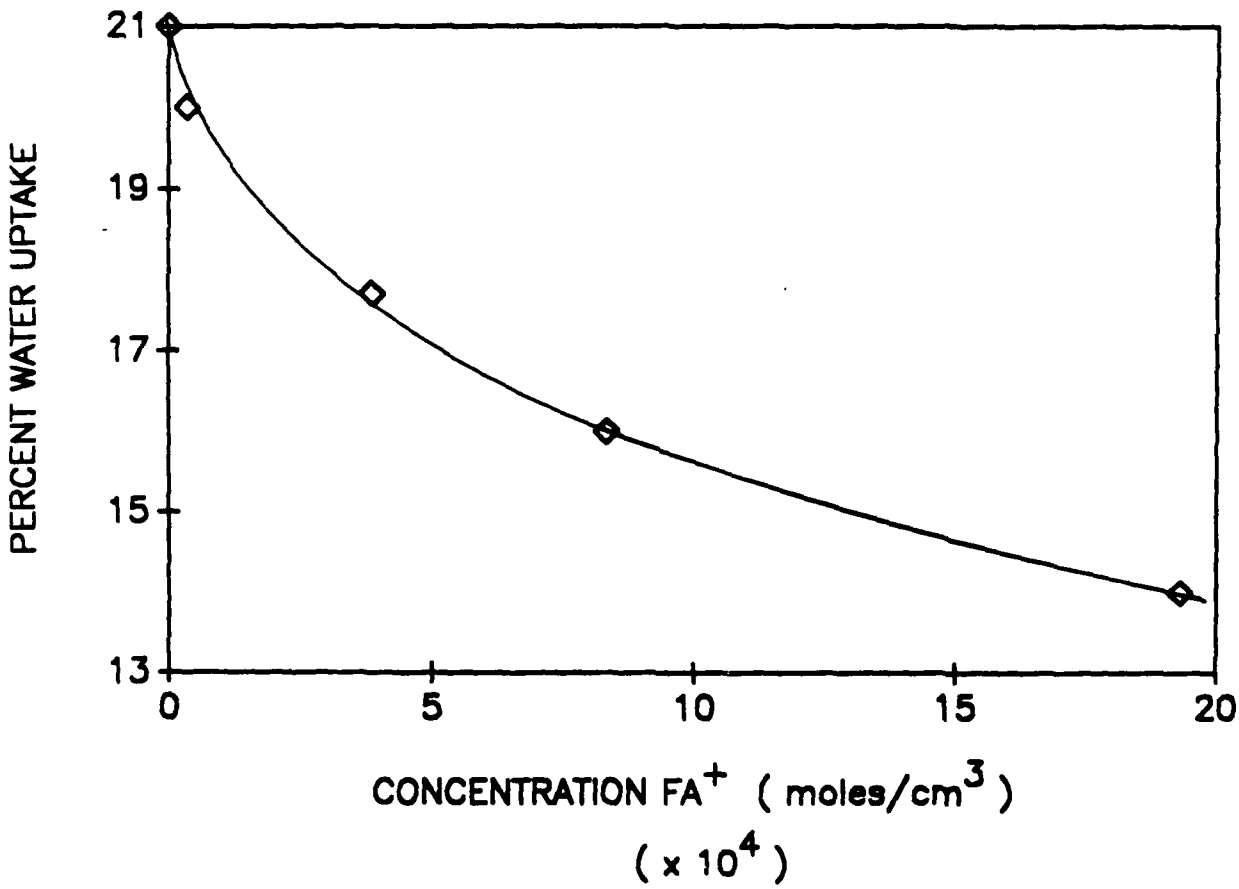
21
19
17
15
13
PERCENT WATER UPTAKE
0
5
10
15
20
CONCENTRATION FA+ (moles/cm3)
(x 10^4)

FIGURE 9